A novel efficient oxide electrode for electrocatalytic oxygen reduction at 400–600 °C†

Wei Zhou, Zongping Shao,* Ran Ran, Wanqin Jin and Nanping Xu

Received (in Cambridge, UK) 31st July 2008, Accepted 9th September 2008
First published as an Advance Article on the web 1st October 2008
DOI: 10.1039/b813327a

A novel $SrNb_{0.1}Co_{0.9}O_{3-\delta}$ electrode material, which possesses not only high electrical conductivity but also large oxygen vacancy concentration at 400–600 °C, shows an excellent performance in the application of reduced temperature solid-oxide fuel cells.

Advanced low-temperature (<600 °C) solid-oxide fuel cells (LTSOFCs) require highly functional cathode materials that can provide high ionic and electronic conductivity and electrocatalytic activity on oxygen reduction reaction to reduce polarization resistance at the cathode/electrolyte interface at low operating temperatures.[1–5] Such functional materials have not been available for many years until $Ba_{0.5}Sr_{0.5}Co_{0.8}Fe_{0.2}O_{3-\delta}$ (BSCF) perovskite was successfully developed as the cathode for SOFCs operating at the temperature below 600 °C.[6,7]

Some interests are focused on further reducing the operating temperature of the SOFC while maintaining a favorable performance. As hardly any single-phase cathode materials possess enough ionic and electronic conductivity simultaneously, second-phase materials are usually added to improve the ionic or electronic conductivity of the cathode.[8–13] However, the issue concerning the compatibility between the multiphase components and the complicated preparation process somewhat restricts their application in practice.[12–14] Very recently, it was reported that the Nb-doping can efficiently stabilize the cubic perovskite crystal structure of $SrCoO_{3-\delta}$ oxide, which is noted for both high oxide ionic and electronic conductivity at elevated temperature. As a result, Nb-doped $SrCoO_{3-\delta}$ perovskite oxides showed high oxygen permeability in the application of the oxygen separation membranes.[14] In this report, we demonstrate for the first time to our knowledge, that single-phase $SrNb_{0.1}Co_{0.9}O_{3-\delta}$ (SNC) is also a potential cathode, which has extremely low polarization resistance at temperatures below 600 °C, accordingly, the peak power density of the fuel cell is improved ~40% as compared with that based on the BSCF cathode at 500 °C.

It is generally accepted that an ideal SOFC cathode should possess high electronic conductivity (100 S cm^{-1}) at the desired operating temperatures. The excessively low electronic conductivity of BSCF (<40 S cm^{-1} in air as shown in Fig. S1, ESI†) seems one of the key problems with respect to the relatively low electrochemical performance at low temperature. This was experimentally verified by the fact that adding silver to BSCF improved the cathode performance significantly at 500 °C.[8] One advantage of SNC is its high electrical conductivity. As shown in Fig. 1, the electrical conductivity of SNC is >100 S cm^{-1} below 525 °C in air. In practical application of a fuel cell, consumption of oxygen is very large at high current density, which leads to oxygen concentration at the inner cathode being much lower than the outer surface of the cathode. As shown in Fig. S1,† the electrical conductivity of BSCF is <10 S cm^{-1} in nitrogen. The oxygen reduction reaction in the BSCF cathode is thus bound to be deteriorated at the cathode–electrolyte–gas interface, the so-called triple-phase boundary (TPB), which is the highly efficient zone for the oxygen reduction. It is exciting that for SNC material that its electrical conductivity can still be as high as ~30 S cm^{-1} in nitrogen, which would supply sufficient electronic conductivity at the vicinity of the TPB.

Another key factor concerning the cathode performance is the oxygen vacancy concentration of the material. Oxygen vacancies supply the active sites for oxygen adsorption, dissociation and diffusion at the material's surface, and passage for oxide ion transport in the material bulk. Fig. 2 compares the oxygen nonstoichiometry (δ) of SNC and BSCF in air as a function of temperature. The initial δ value of SNC is 0.219 at room temperature, which is lower than the value of 0.350 for BSCF. With increased temperature, however, the δ value of SNC grew faster as compared to BSCF, and became higher than that of BSCF at around 450 °C. The higher oxygen vacancy concentration is another advantage for SNC to achieve a high electrochemical performance at low operating temperature.

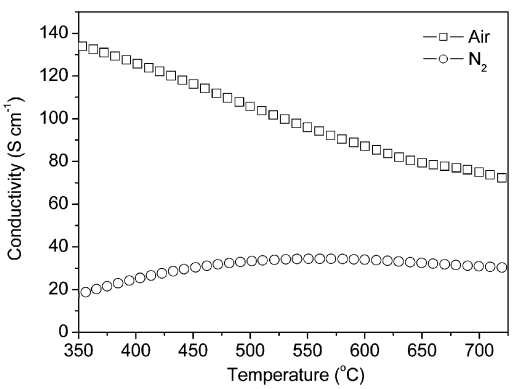

Fig. 1 Electrical conductivity of SNC measured at various temperatures in air and N_2.

State Key Laboratory of Materials-Oriented Chemical Engineering, College of Chemistry and Chemical Engineering, Nanjing University of Technology, No.5 Xin Mofan Road, Nanjing, 210009, P. R. China. E-mail: shaozp@njut.edu.cn; Fax: 86-25-83365813; Tel: 86-25-83587722

† Electronic supplementary information (ESI) available: Experimental section. See DOI: 10.1039/b813327a

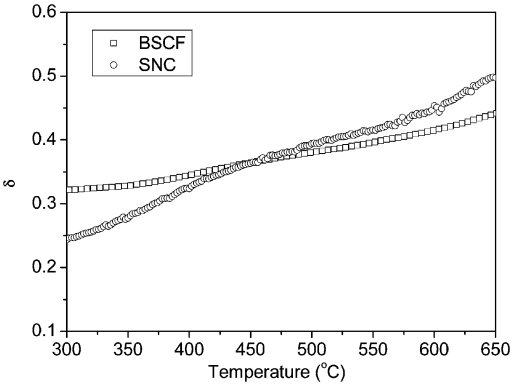

Fig. 2 Temperature dependence of oxygen nonstoichiometry of SNC and BSCF in air.

A symmetric cell with a configuration of SNC|SDC|SNC was first investigated to evaluate the SNC cathode electrochemical performance. Fig. 3 compares the area specific resistances (ASRs) of SNC and BSCF at various temperatures. The ASR of SNC values are 0.040 and 0.094 Ω cm^2 at 650 and 600 °C, respectively, which are very similar to the values of BSCF. As the temperature decreased, the ASRs of SNC increased more slowly than those of BSCF. The ASRs are 0.203, 0.606 and 1.828 Ω cm^2 for SNC at 550, 500 and 450 °C, respectively, while those for BSCF are 0.247, 0.771 and 2.875 Ω cm^2. The activation energy for oxygen reduction on SNC cathode is 105 kJ mol^{-1}, which is also lower than 116 kJ mol^{-1} for BSCF.[6] This suggests that the SNC is a more suitable cathode for SOFC operating at low temperature than BSCF.

SEM micrographs of the SNC and BSCF cathodes are shown in Fig. S2, ESI.†The BSCF particles sintered easily due to the high surface energy, so the cathode shows very large particle sizes. In the case of the SNC cathode, large particles can also be observed. However, there are many fine SNC grains with a particle size as small as ~0.5 μm dispersed on the surface of the large particles, which can increase the effective surface area for oxygen reduction reaction. This may also contribute to the improved performance of the SNC cathode.

Nyquist plots of the cells with the SNC cathode were obtained at 600 °C under various P(O_2), and are given in Fig. S3, ESI.†All the impedance spectra contain two separable depressed arcs, suggesting that at least two different electrode processes limit the oxygen reduction reaction. To obtain a more deep understanding the kinetics of oxygen reduction reaction on SNC, the impedance spectra were evaluated by fitting the impedance spectra to an equivalent circuit with a configuration of $R_{ohm}(R_{E1} - CPE_1)(R_{E2} - CPE_2)$, where R_{ohm} is the overall ohmic resistance including the electrolyte resistance, the electrode ohmic resistance and the lead resistance; and *CPE* is a constant phase element. It was observed that $1/R_{E1}$ had a pO_2 dependent slope of ~1/4 and the $1/R_{E2}$ had a pO_2 dependent slope of ~1/2 for both the SNC and BSCF (Fig. S4, ESI†). The process with a pO_2 dependency of 1/4 could be related to the oxygen reduction reaction accompanying the electron-transfer process, while that with a pO_2 dependency of 1/2 it could be related to the surface diffusion of oxygen atoms or the adsorption of molecular oxygen.[15–17] Both the R_{E1} and R_{E2} of SNC are lower than those of BSCF (Fig. S5, ESI†). This indicates that, for the SNC cathode, the enhanced electrical conductivity accelerated the charge-transfer process, while the higher oxygen vacancy concentration improved surface diffusion or adsorption processes as compared with the BSCF cathode.

Cathode overpotential is an important factor in electrode performances. The IR-corrected Tafel plots for the SNC cathode as a function of temperature are shown in Fig. 4. The polarization overpotential was only −110 mV for SNC cathode at current densities of −1340, −626, −236 and −92 mA cm^{-2} at 600, 550, 500 and 450 °C in air. The high current densities imply that good fuel cell performances could be obtained at lower temperatures.

A complete cell with a 20-μm thick SDC electrolyte and a SDC-Ni (50/50 vol%) anode was tested. Air was supplied to the cathode chamber and humidified H_2 (3% H_2O) to the anode chamber. Fig. 5 shows the cell voltages and power densities at various temperatures. The maximum power density (P_{max}) reached 1008 mW cm^{-2} at 600 °C, which is comparable to those obtained from cells based on advanced cathodes operated under the same conditions.[6,18–20] When the cell worked at the operating temperatures below 600 °C, the values were significantly higher than those reported for SDC-electrolyte fuel cells, *i.e.* 838, 561, 345 and 153 mW cm^{-2} at 550, 500, 450 and 400 °C respectively. The results are much higher than those obtained from the fuel cell based on the BSCF cathode.[6]

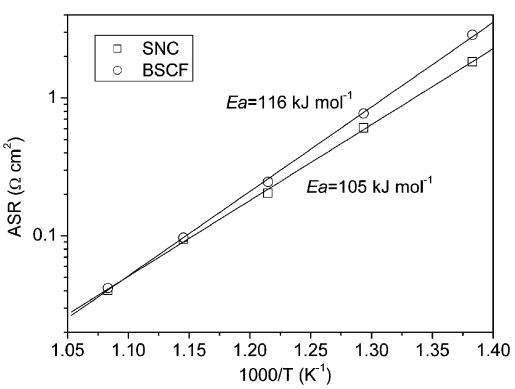

Fig. 3 Temperature dependence of ASRs for SNC and BSCF cathodes.

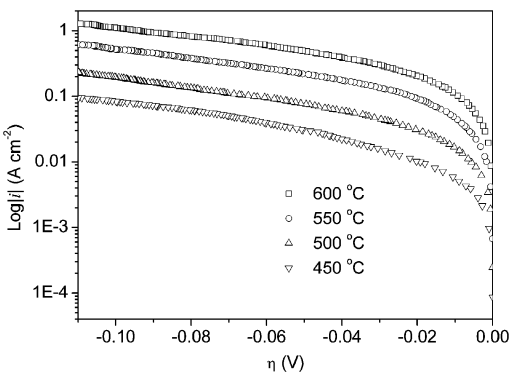

Fig. 4 IR-corrected Tafel plots for SNC cathode as a function of temperature.

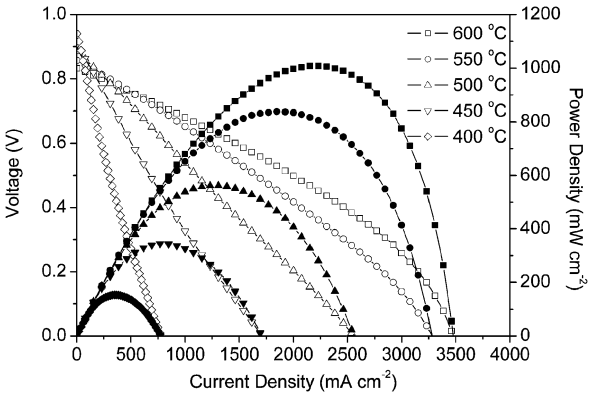

Fig. 5 *I–V* and *I–W* curves for SOFCs with the SNC cathodes.

In summary, single-phase SNC cathode was successfully used as the cathode for an SOFC operated at temperatures below 600 °C. The Nb-doping dramatically increased the electrical conductivity and the oxygen vacancy concentration of the material at the operating temperatures as compared with BSCF. Both characteristics resulted in considerably reduced polarization resistance in both charge-transfer and surface diffusion processes, so leading to much lower total polarization resistance for the SNC cathode. The peak power density reached as high as 561 mW cm^{-2} at 500 °C based on a 20-μm thick SDC electrolyte. The characteristics of both high mixed electronic and ionic conductivity and high oxygen nonstoichiometry of the cathode material also implied their promising potential application in oxygen generator, oxygen sensor and mild oxide catalysts.

This work was supported by the National Natural Science Foundation of China under contract Nos. 20646002, and 20676061, by the National 863 program under contract No. 2007AA05Z133, and by the National Basic Research Program of China under contract No. 2007CB209704.

Notes and references

1 B. C. H. Steele and A. Heinzel, *Nature*, 2001, **414**, 345.
2 T. Hibino, A. Hashimoto, T. Inoue, J. Tokuno, S. Yoshida and M. Sano, *Science*, 2000, **288**, 2031.
3 M. G. Bellino, J. G. Sacanell, D. G. Lamas, A. G. Leyva and N. E. Walsoe de Reca, *J. Am. Chem. Soc.*, 2007, **129**, 3066.
4 C. R. Xia and M. L. Liu, *Adv. Mater.*, 2002, **14**, 521.
5 T. Z. Sholklapper, H. Kurokawa, C. P. Jacobson, S. J. Visco and L. C. De Jonghe, *Nano Lett.*, 2007, **7**, 2136.
6 Z. P. Shao and S. M. Haile, *Nature*, 2004, **431**, 170.
7 Z. P. Shao, S. M. Haile, J. Ahn, P. D. Ronney, Z. L. Zhan and S. A. Barnett, *Nature*, 2005, **435**, 795.
8 W. Zhou, Z. P. Shao, R. Ran, Z. H. Chen, P. Y. Zeng, H. X. Gu, W. Q. Jin and N. P. Xu, *Electrochim. Acta*, 2007, **52**, 6297.
9 W. Zhou, Z. P. Shao, R. Ran, P. Y. Zeng, H. X. Gu, W. Q. Jin and N. P. Xu, *J. Power Sources*, 2007, **168**, 330–337.
10 W. Zhou, R. Ran, Z. P. Shao, R. Cai, W. Q. Jin, N. P. Xu and J. Ahn, *Electrochim. Acta*, 2008, **53**, 4370.
11 K. Wang, R. Ran, W. Zhou, H. X. Gu, Z. P. Shao and J. Ahn, *J. Power Sources*, 2008, **179**, 60.
12 R. Su, Z. Lü, K. F. Chen, N. Ai, S. Y. Li, B. Wei and W. H. Su, *Electrochem. Commun.*, 2008, **10**, 844.
13 Y. S. Wang, S. R. Wang, Z. R. Wang, T. L. Wen and Z. Y. Wen, *J. Alloys Compd.*, 2007, **428**, 286.
14 T. Nagai, W. Ito and T. Sakon, *Solid State Ionics*, 2007, **177**, 3433.
15 X. J. Chen, S. H. Chan and K. A. Khor, *Electrochim. Acta*, 2004, **49**, 1851.
16 M. J. Jørgensen and M. Mogensen, *J. Electrochem. Soc.*, 2001, **148**, A433.
17 M. Koyama, C. Wen, T. Masuyama, J. Otomo, H. Fukunaga, K. Yamada, K. Eguchi and H. Takahashi, *J. Electrochem. Soc.*, 2001, **148**, A795.
18 W. Zhou, R. Ran, Z. P. Shao, W. Zhuang, J. Jia, H. X. Gu, W. Q. Jin and N. P. Xu, *Acta Mater.*, 2008, **56**, 2687.
19 W. Zhou, R. Ran, Z. P. Shao, H. X. Gu, W. Q. Jin and N. P. Xu, *J. Power Sources*, 2007, **174**, 237.
20 W. Zhou, R. Ran, Z. P. Shao, W. Q. Jin and N. P. Xu, *J. Power Sources*, 2008, **182**, 24.